

## Dust-ion acoustic shock waves for nonplanar geometry with nonthermal electrons and adiabatic dusty plasma

Louis Ete AKPABIO\*

Theoretical Physics Group, Department of Physics, University of Uyo, Uyo, Nigeria

Received: 14.11.2014

Accepted/Published Online: 23.06.2015

Printed: 30.11.2015

**Abstract:** The nonplanar Burgers' equation for dust-ion-acoustic shock waves was derived for unmagnetized adiabatic dusty plasmas, comprising static negatively charged dust fluid, nonthermal distributed electrons, and Boltzmann distributed positron and adiabatic ion fluid, by employing the standard reductive perturbation method. The solution of the modified Burgers' equation for nonplanar geometry is numerically analyzed. The dependence of dust-ion-acoustic shock waves on some plasma parameters is explored. It is observed that inclusion of the nonthermal electron distribution modifies the shock wave profile significantly. Likewise, it is found that the nonplanar geometry effects have an important role on the establishment of shock waves. It is also found that an increasing positron concentration decreases the amplitude of the dust-ion-acoustic shock waves.

**Key words:** Dust-ion-acoustic shock, nonplanar geometry, multicomponent adiabatic dusty plasma, nonthermal electrons

### 1. Introduction

Fully ionized gases consisting of electrons and positrons of equal masses and ions are usually characterized as electron-positron-ion plasma [1]. The pressure of ions brings about the existence of several low-frequency waves, which otherwise do not propagate in electron-positron plasmas. The interplay between charged dust grains and plasma has led to much interest in a new research area called dusty (or complex) plasma. Linear as well as nonlinear collective processes in dusty or complex plasmas have received special attention due to the realization of their occurrence in planetary rings, interstellar clouds, and cometary environments [2–7]. There has been rapidly growing interest in nonlinear phenomena (such as shocks, solitons, and vortices) in dusty plasma (plasmas with extremely massive and negatively charged dust grains) because of its crucial role in understanding electrostatic disturbance in space and laboratory dusty plasmas [8–12]. It is obvious that the presence of statically charged dust grains modifies the existing plasma wave spectra [13–15].

Numerous studies have clearly indicated the presence of energetic (nonthermally/suprathermally) electrons in a variety of astrophysical plasma environments and measurements of their distribution functions, and have shown them to be highly nonthermal [16]. The nonthermal electron and ion distributions [17–19] are turning out to be characteristic features of space plasma, where structures like solitons, shocks, double layers, vortices, etc. are expected to play important roles. Since the electron and ion distributions play important roles for the formation of nonlinear structures, it is interesting to study the coherent nonlinear wave structures with non-Maxwellian distribution of electrons/ions. Most of the astrophysical plasmas usually contain highly

\*Correspondence: louisakpabio@uniuyo.edu.ng

charged (negative/positive) impurities or dust particulates in addition to the electrons, positrons, and ions. However, the properties of wave motions of electron-positron-ion-dust plasma should be different from those in three-component electron-positron-ion plasmas [20–22].

Dust-ion-acoustic shock waves in an unmagnetized dusty plasma may arise owing to the interplay between nonlinearity (associated with the harmonic generation) and the dust-ion drag. The formation of a dust-ion-acoustic shock wave (DIASW) was observed by Nakamura et al. [23]. They discovered that both monotonic and oscillatory shock waves exist and the dust density has a vital role in the shock waves and phase velocity of the wave. A number of papers by several investigators have shed light on the properties of DIASWs in dusty plasma [24–27].

Recently, Sahu [28] carried out a theoretical investigation of the effect of nonplanar DIASWs in adiabatic dusty plasma. The objective of the present investigation is to study the nonlinear propagation of DIASWs in multicomponent adiabatic dusty plasma comprising electrons, positrons, ions, and dust respectively in a nonplanar geometry. In this regard, Burgers' equation is derived using the reductive perturbation method (RPM). Hence, we have analyzed the DIASWs in nonplanar geometry showing how the inclusion of nonthermal electron distribution gets the shock wave structure modified. We have also studied the effect of increasing positron concentration on the propagation of DIASWs in nonplanar geometry. The paper is organized in the following manner: the basic equations governing the adiabatic dusty plasma system under consideration are given and the nonplanar Burgers' equation is derived in Section 2. In Section 3, we discuss the numerical results, and Section 4 gives the conclusion.

## 2. Basic equations and derivation of nonplanar Burgers' equation

A four-component unmagnetized plasma comprises static negatively charged dust fluid, nonthermal distributed electrons, Boltzmann distributed positrons, and adiabatic ion fluid. The dynamic of the DIASWs in nonplanar geometry for such dusty plasma is governed by the following normalized fluid equations.

$$n_i \frac{\partial n}{\partial t} + \frac{1}{r^\nu} \frac{\partial}{\partial r} (r^\nu n_i u_i) = 0 \quad (1)$$

$$n_i \frac{\partial u_i}{\partial t} + n_i u_i = -n_i \frac{\partial \varphi}{\partial r} - \alpha \frac{\partial p_i}{\partial r} + \eta_i n_i \left[ \frac{1}{r^\nu} \frac{\partial}{\partial r} \left( r^\nu \frac{\partial u_i}{\partial r} \right) - \frac{\nu u_i}{r^\nu} \right] \quad (2)$$

$$\frac{\partial p_i}{\partial t} + u_i \frac{\partial p_i}{\partial r} + 3p_i \frac{1}{r^\nu} \frac{\partial}{\partial r} (r^\nu u_i) = 0 \quad (3)$$

$$\mu \exp(\varphi) (1 - \beta\varphi + \beta\varphi^2) - \delta_p \exp(-\varphi) - n_i + \left( \delta_p + \frac{1}{1 + \mu} \right) = 0 \quad (4)$$

Here,  $\beta = \frac{4\alpha_1}{1+3\alpha_1}$ ;  $\alpha_1$  is parameter determining the number of nonthermal electrons present in our plasma model.

In the above equation,  $n_i$  is the ion number density normalized by its equilibrium value  $n_{i0}$ ,  $u_i$  is the ion fluid speed normalized by  $c_i = (K_B T_e / m_i)^{1/2}$ ,  $\varphi$  is the wave potential normalized by  $K_B T_e / e$ ,  $p_i$  is the ion thermal pressure normalized by  $n_{i0} K_B T_i$ ,  $\alpha = T_i / T_e$ . The time and space variable are normalized by reciprocal plasma frequency  $\omega_{pi}^{-1} = (m_i / 4\bar{n} n_{i0} e^2)^{1/2}$  and the Debye length  $\lambda_D = (K_B T_e / 4\bar{n} n_{i0} e^2)^{1/2}$ , respectively, while  $\nu = 0$  for one-dimensional geometry and  $\nu = 1, 2$  for cylindrical and spherical geometry, respectively.  $\eta_i$  is

the viscosity coefficient of ion fluid normalized by  $w_{p_i} \lambda_D^2$ ,  $\mu = n_{e0}/n_{i0}$ , and  $\delta_p = n_{p0}/n_{i0}$ . In Eq. (4), we have assumed the quasineutrality condition.

Employing the RPM and stretched coordinates  $\xi = \epsilon^{1/2} (r - V_0 t)$  and  $\tau = \epsilon^{3/2} t_i$ , we derive Burgers' equation from Eqs. (1)–(4) in terms of  $\xi$  and  $\tau$  as follows.

$$\epsilon^{3/2} \partial_\tau n_i - V_0 \epsilon^{1/2} \partial_\xi n_i + \epsilon^{1/2} \partial_\xi (n_i u_i) + \frac{\nu \epsilon^{3/2}}{V_0 \tau \left(1 + \frac{\xi \epsilon}{V_0 \tau}\right)} (n_i u_i) = 0 \quad (5)$$

$$\begin{aligned} & \epsilon^{3/2} n_i \partial_\tau u_i - V_0 \epsilon^{1/2} n_i \partial_\xi u_i + \epsilon^{1/2} n_i u_i \partial_\xi u_i = -\epsilon^{1/2} n_i \partial_\xi \varphi_1 \\ & -\epsilon^{1/2} \alpha \partial_\xi p_i + \epsilon^{1/2} \eta_0 n_i \left[ \epsilon^2 \partial_\xi^2 u_i + \frac{\nu \epsilon^2}{V_0 \tau \left(1 + \frac{\xi \epsilon}{V_0 \tau}\right)} \partial_\xi u_i - \frac{V \epsilon^3}{V_0^2 \tau^2 \left(1 + \frac{\xi \epsilon}{V_0 \tau}\right)^2} u_i \right] = 0 \end{aligned} \quad (6)$$

$$\epsilon^{3/2} \partial_\xi p_i - V_0 \epsilon^{1/2} \partial_\xi p_i + \epsilon^{1/2} u_i \partial_\xi p_i + 3p_i \left[ \epsilon^{1/2} \partial_\xi u_i + \frac{\nu \epsilon^{3/2}}{V_0 \tau \left(1 + \frac{\xi \epsilon}{V_0 \tau}\right)} u_i \right] = 0 \quad (7)$$

$$\mu \left(1 + \varphi + \frac{1}{2} \varphi^2 + \dots\right) (1 - \beta \varphi + \beta \varphi^2) - \delta_p \left(1 - \varphi + \frac{1}{2} \varphi^2 - \dots\right) - n_i + \left(\delta_p + \frac{1}{1 + \mu} = 0\right) \quad (8)$$

Here,  $\epsilon$  is a smaller parameter measuring the weakness of the nonlinearity,  $V_0$  is the phase speed of DIASWs normalized by  $C_i$ , and  $\eta = \epsilon^{1/2} \eta_0$  is assumed [29]. The dependent variables  $n_i$ ,  $u_i$ ,  $p_i$ , and  $\varphi$  are expanded in a power series of  $\epsilon$  as follows.

$$\left. \begin{aligned} n_i &= 1 + \epsilon n_{i1} + \epsilon^2 n_{i2} + \dots \\ u_i &= 0 + \epsilon u_{i1} + \epsilon^2 u_{i2} + \dots \\ p_i &= 1 + \epsilon p_{i1} + \epsilon^2 p_{i2} + \dots \\ \varphi &= 0 + \epsilon \varphi_1 + \epsilon^2 \varphi_2 + \dots \end{aligned} \right\} \quad (9)$$

Now, substituting Eq. (9) into Eqs. (5)–(8), we obtain the lowest order of the coefficient of  $\epsilon$  as follows.

$$n_{i1} = [(1 - \beta) \mu + \delta_p] \varphi_1 \quad (10)$$

$$u_{i1} = V_0 [(1 - \beta) \mu + \delta_p] \varphi_1 \quad (11)$$

$$p_{i1} = 3 [(1 - \beta) \mu + \delta_p] \varphi_1 \quad (12)$$

$$V_0 = \sqrt{3\alpha + 1/(1 - \beta) \mu + \delta_p} \quad (13)$$

The next higher order in  $\epsilon$  is as given below.

$$\partial_\tau n_{i1} - V_0 \partial_\xi n_{i2} + \partial_\xi (n_{i1} u_{i1}) + \partial_\xi u_{i2} + \frac{v u_{i1}}{V_0 \tau} = 0 \quad (14)$$

$$\partial_\tau u_{i1} - V_0 \partial_\xi u_{i2} + u_{i1} \partial_\xi u_{i1} - V_0 n_{i1} \partial_\xi u_{i1} + \alpha \partial_\xi p_{i2} = -\partial_\xi \varphi_2 - n_{i1} \partial_\xi \varphi_1 + \eta_0 \partial_\xi^2 u_{i1} \quad (15)$$

$$\partial_\xi p_{i1} - V_0 \partial_y p_{i2} + u_{i1} \partial_\xi p_{i1} + 3 \partial_\xi u_{i2} + 3 p_{i1} \partial_\xi u_{i1} + \frac{3 v u_{i1}}{V_0 \tau} = 0 \quad (16)$$

$$n_{i2} = \{\mu(1 - \beta) + \delta_p\} \varphi_2 + \frac{1}{2} \{\mu(1 - \beta) + \delta_p\} \varphi_1^2 \quad (17)$$

Using Eqs. (10)–(17) and eliminating  $n_{i2}$ ,  $u_{i2}$ ,  $p_{i2}$ , and  $\varphi_2$ , we finally obtain a modified Burgers' equation as:

$$\partial_\tau \varphi_1 + \frac{v\varphi_1}{2\tau} + A\varphi_1 \frac{\partial \varphi_1}{\partial \xi} - C \frac{\partial^2 \varphi_1}{\partial \xi^2} = 0, \quad (18)$$

where:

$$A = \frac{12\alpha[(1 - \beta)\mu + \delta_p]^2 + 3[(1 - \beta)\mu + \delta_p] - 1}{2(\sqrt{3\alpha + 1/(1 - \beta)\mu + \delta_p})((1 - \beta)\mu + \delta_p)} \quad (19)$$

$$C = \eta_0/2 \quad (20)$$

### 3. Numerical results and discussion

The modified Burgers' equation as given in Eq. (18) describes the nonlinear propagation of the DIASWs for a four-component unmagnetized dusty plasma comprising static negatively charged dust fluid, nonthermal distributed electrons, Boltzmann distributed positrons, and adiabatic ion fluid. The stationary DIASWs of this modified Burgers' equation for planar geometry ( $v = 0$ ) is as follows.

$$\varphi_1 = \frac{V}{A} \left[ 1 - \tanh \left( \frac{V(\xi - V\tau)}{2C} \right) \right] \quad (21)$$

Here,  $V$  is a constant velocity normalized by  $c_i$ . For nonplanar geometry Eq. (18) is not possible; hence, it is solved numerically. The results are displayed in Figures 1–7. The initial condition that we have considered for all our numerical results is the form of the stationary solution of Eq. (21) without the geometry term at  $\tau = -10$ . Figure 1 shows the evolution of the shock wave structures for different geometries with respect to the considered parameters. It is obvious that the developed shock amplitude in different geometries are different from each other, while the shock steepness is the same for all geometries. The planar geometry shock wave with higher amplitude is the strongest. The cylindrical shock wave amplitude is bigger than that of the spherical shock wave but smaller than that of the planar geometry shock wave.

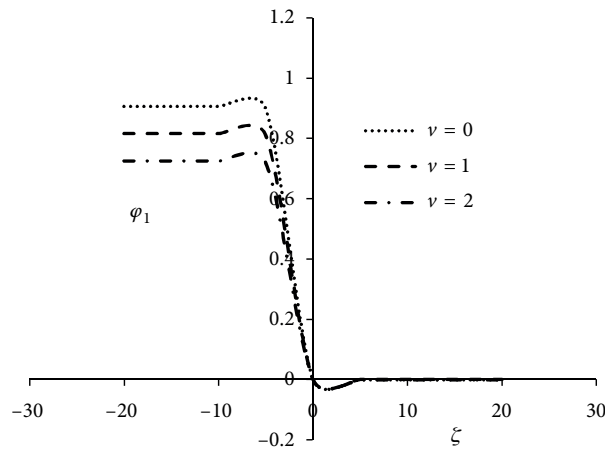


**Figure 1.** How the shock profile ( $\varphi_1 V_s \xi$  curves) varies in different geometries for  $\tau = -5$ ,  $\eta_0 = 0.5$ ,  $\alpha = 0.5$ ,  $\beta = 0.3$ ,  $\mu = 0.4$ , and  $\delta_p = 0.3$ .

The variation of cylindrical and spherical shock wave structures for different  $\tau$  with respect to the chosen parameters are plotted in Figures 2 and 3, respectively. We can observe that as time increases ( $\tau$ ), the amplitude of the nonplanar geometry (Figures 2 and 3) shock waves also increases. It can also be observed that the shock wave profiles for the nonplanar geometry (Figures 2 and 3) are similar to what is obtained for the planar geometry of Figure 1 in terms of the amplitude for larger values of  $|\tau|$ . This result confirms the fact that the large value of the nonplanar geometrical effect ( $\frac{v}{2\tau}$ ) is no longer dominant. The nonplanar geometrical effects will become effective as the value of  $\tau$  decreases. The effect of positron concentration on the shock wave structures for cylindrical and spherical geometries are presented in Figures 4 and 5, respectively. To study the effect of positron concentration in the DIASWs, we set  $\beta = 0.01$  for Figures 4 and 5, while other parameters for the numerical analysis are as obtained in Figures 1–3. From Figures 4 and 5, it is found that increase in positron concentration decreases the amplitude of the DIASWs for nonplanar geometry. In physical situations, it is obvious that any increase in positron concentration decreases the ion concentration. Since we are dealing with DIASWs, the amplitude of the shock structures will decrease for increase in positron concentration. The effects of nonthermal electron distribution parameter ( $\beta$ ) on shock wave are also studied. In Figures 6 and 7, we present the plot of the shock wave structures for different values of  $\beta$  in the cylindrical and spherical geometry, respectively. It is clear that small variations in the magnitude of  $\beta$  significantly affect the shock wave profile. The shock height is found to be increasing monotonically with  $\beta$ . This effect is found to be more pronounced in the cylindrical geometry (Figure 6) compared to the spherical geometry (Figure 7).

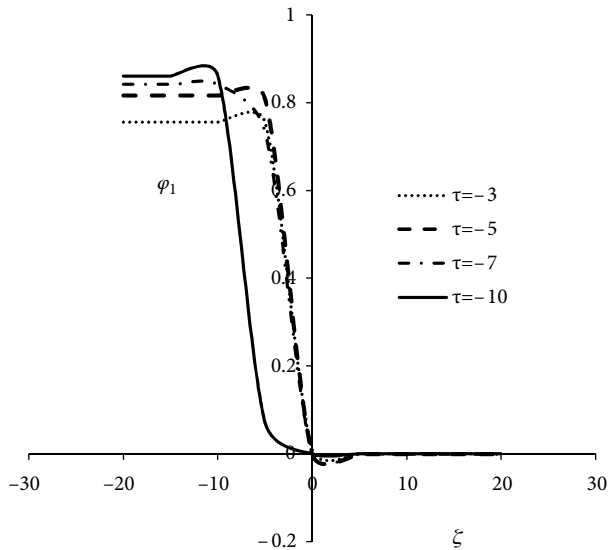


**Figure 2.** Variation of  $\varphi_1$  with respect to  $\xi$  at different values of  $\tau$  for the cylindrical geometry ( $v = 1$ ) while other parameters are the same as in Figure 1.

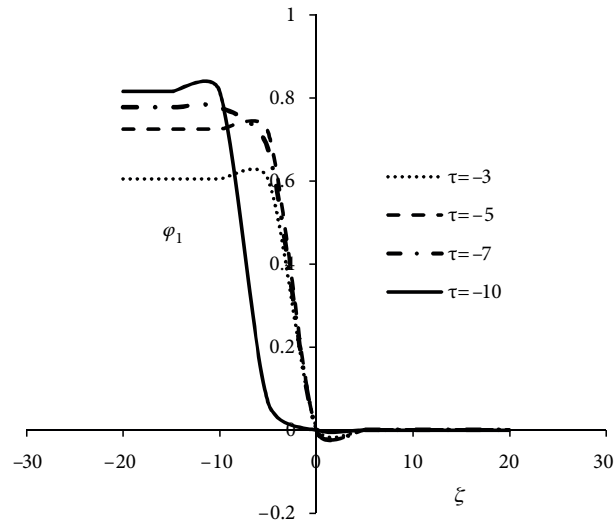


**Figure 3.** Variation of  $\varphi_1$  with respect to  $\xi$  at different values of  $\tau$  for the spherical geometry ( $v = 2$ ) while other parameters are the same as in Figure 1.

#### 4. Conclusion

We have derived the nonplanar Burgers' equation for dust-ion-acoustic shock waves in unmagnetized adiabatic dust plasma, comprising static negatively charged dust fluid, nonthermal electron distribution, Boltzmann distributed positrons, and adiabatic ion fluid, by employing the standard RPM.

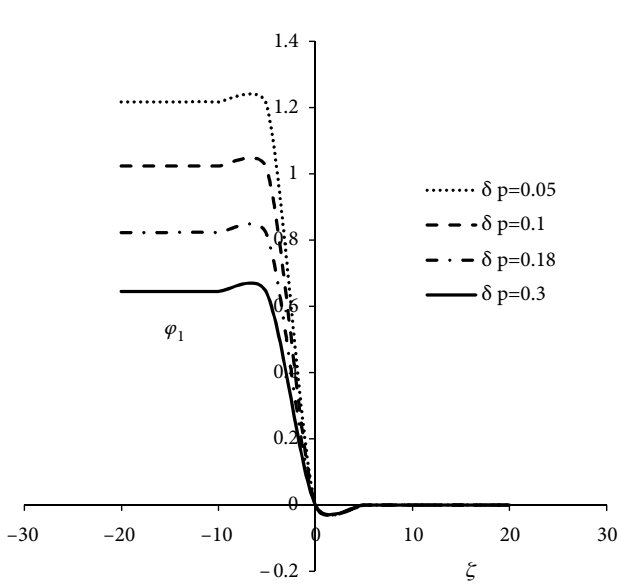


**Figure 4.** Variation of  $\varphi_1$  with respect to  $\xi$  at different values of the positron concentration for  $\beta = 0.01$  in the cylindrical geometry ( $v = 1$ ) while other parameters are the same as in Figure 1.

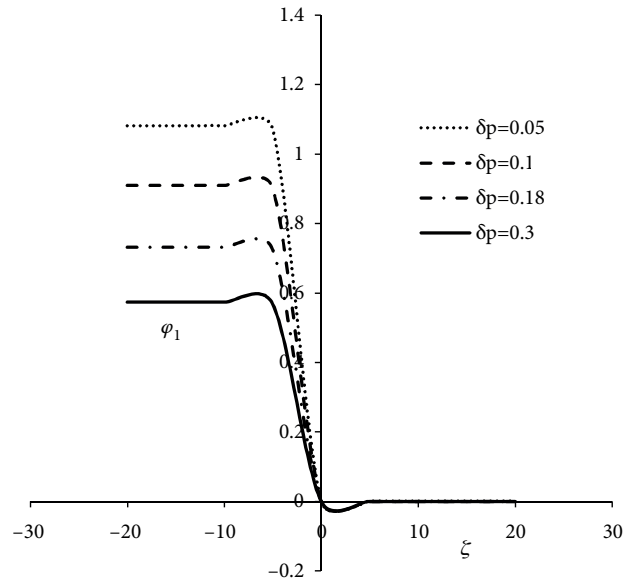


**Figure 5.** Variation of  $\varphi_1$  with respect to  $\xi$  at different values of the positron concentration for  $\beta = 0.01$  in the spherical geometry ( $v = 2$ ) while other parameters are the same as in Figure 1.

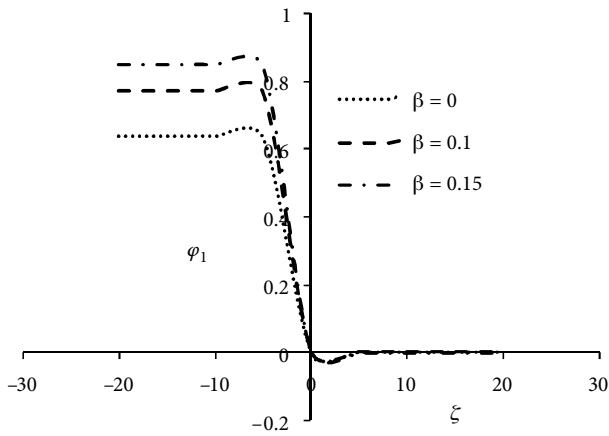


**Figure 6.** Variation of  $\varphi_1$  with respect to  $\xi$  at different values of the nonthermal electron parameter ( $\beta$ ) for the cylindrical geometry ( $v = 1$ ) while other parameters are the same as in Figure 1.

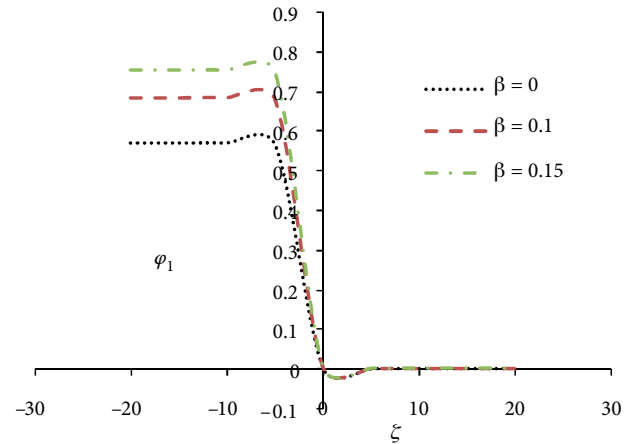


**Figure 7.** Variation of  $\varphi_1$  with respect to  $\xi$  at different values of the nonthermal electron parameter ( $\beta$ ) for the spherical geometry ( $v = 2$ ) while other parameters are the same as in Figure 1.

We have found that the propagation of DIASWs in nonplanar geometry with the inclusion of nonthermal electron distribution modifies the shock wave structure, as the shock profile is found to vary significantly with the nonthermal parameter  $\beta$ . This effect is more prominent in the cylindrical geometry as compared to the spherical geometry. It is also observed that the shock height increases monotonically with the nonplanar geometry. For large negative values of  $\tau$ , it is observed that the nonplanar geometries approach the planar geometry.

Finally, increasing positron concentrations decrease the amplitude of the DIASWs. The present investigation may be very vital in the understanding of the nonlinear propagation characteristic of DIASWs that are necessary in laboratory plasma as well as in plasma applications.

### References

- [1] Tandberg-Hansen, E.; Emusle, A. G. *The Physics of Solar Flares*; Cambridge University Press, Cambridge, UK, 1988.
- [2] Shukla, P. K. *Phys. Plasmas* **2001**, *8*, 1791–1803.
- [3] Bliokh, P.; Sinitsin, V.; Yaroshenko, V. *Dusty and Self-Gravitational Plasma in Space*; Kluwer Academic, Dordrecht, the Netherlands, 1995.
- [4] Shukla, P. K.; Mendis, D. A.; Chow, V. W. *The Physics of Dusty Plasma*; World Scientific, Singapore, 1996.
- [5] Mendis, D. A.; Rosenberg, M. *IEEE T. Plasma Sci.* **1992**, *20*, 929–938.
- [6] Mendis, D. A. In *Advances in Dusty Plasma*; Shukla, P. K.; Mendis, D. A.; Desei, T., Eds. World Scientific, Singapore, 1997, pp. 3–19.
- [7] Verheest, F. *Waves in Dusty Space Plasmas*; Kluwer Academic, Dordrecht, the Netherlands, 2000.
- [8] George, C. K. *Rev. Geophys.* **1989**, *27*, 271–282.
- [9] Mendis, D. A.; Rosenberg, M. C. *Annu. Rev. Astrophys.* **1994**, *32*, 419–427.
- [10] D'Angelo, N. *Space Sci.* **1990**, *38*, 1142–1146.
- [11] Barkan, A.; D'Angelo, N.; Merlino, R. L. *Phys. Rev. Lett.* **1994**, *73*, 3093–3096.
- [12] Barkan, A.; Merlino, R. L.; D'Angelo, N. *Phys. Plasmas* **1995**, *2*, 3563–3565.
- [13] Bliokh, P. V.; Yaroshenko, V. V. *Sov. Astron.* **1985**, *29*, 330–336.
- [14] De Angelis, U.; Formisano, V.; Giordano, M. *J. Plasma Phys.* **1988**, *40*, 399–406.
- [15] Shukla, P. K.; Silin, V. P. *Phys. Scripta* **1992**, *45*, 508–513.
- [16] Goldman, M. V.; Oppenheim, M. M.; Newman, D. L. *Nonlinear Proc. Geophys.* **1999**, *6*, 221–226.
- [17] Ghosh, S.; Bharuthram, R.; Khan, M.; Gupta, M. R. *Phys. Plasmas* **2004**, *11*, 3602–3609.
- [18] Roychoudhury, R. *J. Plasmas Phys.* **2002**, *67*, 199–204.
- [19] Maharaja, S. K.; Pillary, S. R.; Bharuthram, R.; Reddy, R. V.; Singh, S. V.; Lakhina, G. S. *J. Plasma Phys.* **2006**, *72*, 43–47.
- [20] Rizzato, F. B. *J. Plasma Phys.* **1988**, *40*, 289–293.
- [21] Berezhiani, V. I.; El-Ashry, M. Y.; Mofize, U. A. *Phys. Rev.* **1994**, *E50*, 448–452.
- [22] Popel, S. I.; Vladimirov, S. V.; Shukla, P. K. *Phys. Plasmas* **1995**, *2*, 716–719.
- [23] Nakamura Y.; Bailung, H.; Shukla, P. K. *Phys. Rev. Lett.* **1999**, *83*, 1602–1607.
- [24] Shukla, P. K.; Mamun, A. A. *Introduction to Dusty Plasma Physics*; IOP Publishing Ltd., Bristol, UK, 2002.
- [25] Shukla, P. K.; Mamun, A. A. *New J. Phys.* **2003**, *5*, 17.1–17.37.
- [26] Rahman, A.; Saiyed, F.; Mamun, A. A. *Phys. Plasmas* **2007**, *14*, 034503.
- [27] Mamun, A. A.; Shukla, P. K. *Geophys. Res. Lett.* **2002**, *29*, 1870.
- [28] Sahu, B. *Bulg. J. Phys.* **2011**, *38*, 175–183.
- [29] Shukla, P. K. *Phys. Plasmas* **2000**, *7*, 1044–1048.